Abstract

The socioeconomic losses from the recent unprecedented incidents in the electric power systems suggest the need for alternative planning strategies that account for the expected and extreme events that are less likely to occur. Such high impact low probability (HILP), or black swan, events are typically weather-related, have accounted for billions of dollars in economic losses, and left customers in the dark for several days. Furthermore, the proliferation of distributed energy resources (DERs) on the distribution grid indicates that system operators can also plan resilience from the customer's end, forming intentional microgrid islands when needed. However, existing planning strategies only minimize the expected operating cost and do not explicitly include the risk of extreme events. With the increasing frequency of black swan events in the current scenario, system operators should focus on the HILP events and find the optimal trade-off decision to maximize resilience with available resources. This proposal aims to investigate the impact of extreme weather events, hurricanes, and floods, on the power grid and propose planning solutions to enhance the grid's resilience. Firstly, we propose a modeling framework to assess the spatiotemporal compounding effect of hurricanes and storm surges on electric power systems. The spatiotemporal probabilistic loss metric helps system operators identify the potential impact and vulnerable components as the storm approaches. Secondly, we develop a risk-averse two-stage stochastic optimization framework for resilience planning of power distribution systems against extreme weather events. The resource planning strategy involves minimizing a risk metric, conditional value-at-risk (CVaR) while adhering to budget constraints for planning. The main idea is to identify a trade-off between risk-averse and risk-neutral planning solutions to maximize the energization of critical loads when a HILP event is realized. The problem is also extended to determine the trade-off among different resources when system operators have a limited budget. This facilitates the selection of specific resources from a portfolio of various resources that can optimally restore critical loads during the realization of a HILP event. In the future, the work will be extended to a larger and broader landscape with an analysis based on realistic extreme weather events and their impact on the power system. The goal will be to create a generic simulation platform capable of generating and assessing the impact of such events on the electric power grid. The work will also include large-scale integrated operational solutions to enhance the resilience of future power grids. Furthermore, advanced parallel algorithms based on dual decomposition methods will be explored for scalable implementation of stochastic programming problems.

Contents

1 Motivation

Optimal power flow (OPF) methods have become vital for efficiently managing distributed energy resources (DERs) such as photovoltaic (PV) and battery energy storage systems (BESS) at the grid edge, aiming to enhance system-level objectives including reliability, resilience, and cost-effectiveness [1, 2]. BESS, by mitigating the fluctuations of intermittent DERs, transforms the OPF problem from a classic single-period formulation into a multi-period, time-coupled optimization that demands intricate modeling and advanced computational methods [1, 3].

Centralized OPF (COPF) approaches typically rely on non-convex formulations—often based on the nonlinear branch flow model [4]—to coordinate controllable devices. Although such methods can provide accurate solutions for small networks [1, 3, 5], computational time and scalability issues limit their utility in large-scale, real-world systems. Metaheuristic and evolutionary algorithms [6] offer alternative solutions but generally struggle with local optimality and slow convergence, especially for high-dimensional multi-period OPF tasks.

To improve tractability, convex relaxations and linear approximations such as LinDistFlow [7] have been widely employed [1, 3, 7]. These methods deliver fast convergence but introduce non-negligible optimality gaps, particularly as network size and DER/BESS penetration increase, which has not been fully quantified in existing research [1]. Recent studies have highlighted this gap, advocating for a systematic comparison of non-convex and linearized frameworks across varied network conditions [1, 7].

Recognizing the limitations of centralized and linear-programming-based solutions, recent research—including our own—has focused on spatial and temporal decomposition for scalable multi-period OPF. Our group adapted the Equivalent Network Approximation (ENApp) framework to enable distributed MPOPF (MPDOPF) in battery-integrated networks, leveraging spatial partitioning to allow parallel solution of local OPF subproblems and reduce global computational burdens [8]. This approach harnesses the radial structure of distribution networks and significantly accelerates convergence while maintaining solution fidelity. Moreover, our models introduce a battery loss term exclusively in the objective function, preventing simultaneous charge/discharge operations and preserving problem convexity without integer variables [8].

Extensive validation against industry-standard IEEE test systems demonstrates that our ENApp-based distributed MPOPF delivers superior scalability and optimality compared with conventional centralized frameworks. These studies also provide a robust, side-by-side comparison of LinDistFlow and branch flow-based nonlinear models for MPOPF across real

distribution network scenarios [1].

Major remaining research gaps include the scalability and real-time applicability of centralized MPOPF approaches [3, 5, 9–11], and the slow convergence and master controller dependencies in existing distributed frameworks such as Benders decomposition [**?**]. The contribution of this work is the development and benchmarking of a spatially distributed multi-period OPF algorithm, overcoming these challenges and enabling practical, accurate, large-scale coordinated grid-edge resource management.

2 Objectives and Task Lists

The overarching goal of this work is to develop a computationally scalable framework for solving the Multi-Period Optimal Power Flow (MPOPF) problem in active distribution systems. The proposed framework aims to address the inherent complexity and non-convexity of MPOPF formulations – arising from temporal coupling of decision variables and high-dimensional system models – by designing and implementing decomposition-based algorithms. The resulting framework is expected to enable tractable and near-optimal solutions for realistic time horizons and large distribution feeders, while preserving the physical fidelity of the underlying models. The following tasks have been completed or are currently being pursued toward achieving the objectives of this study:

1. **Literature Review on Multi-Period Optimal Power Flow:** A comprehensive review was conducted on existing formulations of the MPOPF problem for active distribution systems. This provided insights into modeling temporal dependencies, handling storage dynamics, and integrating distributed energy resources in multi-period settings.

2. **Study of Decomposition-Based Optimization Techniques:** A review of decomposition algorithms, including Bilevel optimization methods, ADMM, and Differential Dynamic Programming (DDP), was carried out to understand their suitability for large-scale and temporally coupled optimization problems. The study highlighted key convergence properties and trade-offs between spatial and temporal decompositions.

3. **Implementation of Spatial Decomposition for MPOPF:** A spatially decomposed MPOPF formulation was implemented and tested on benchmark distribution systems. The method demonstrated improved scalability compared to monolithic optimization, though it remained limited in addressing the temporal coupling present in long-horizon studies.

4. **Development and Evaluation of Differential Dynamic Programming (DDP):** The DDP algorithm was formulated and implemented for the MPOPF problem. While the approach yielded solutions close to those obtained from brute-force optimization, it exhibited oscillatory convergence behavior and lacked strong theoretical guarantees. Further research is required to enhance its stability and convergence properties.

5. **Implementation of Temporal ADMM for MPOPF:** A temporal Alternating Direction Method of Multipliers (ADMM) approach is being developed to address the

scalability challenges associated with increasing time horizons. Preliminary results on a copper-plate system show excellent convergence, and current efforts focus on extending the implementation to LinDistFlow-based distribution models.

6. **Validation and Scalability Testing:** The final phase will involve validating the proposed algorithms on a large-scale system like the 9500-node (three-phase) feeder. The goal is to demonstrate the framework's scalability for realistic horizons (e.g., $T = 96$ i.e. 1 day at 15-minute intervals) and its applicability to operational optimization in distribution grids.

7. **Exploratory Study on Multiple-Source Optimal Power Flow (MS-OPF):** As a future research direction, the framework will be extended to accommodate multi-source configurations, enabling coordinated optimization across multiple substations and zones in distribution networks.

3 Temporal Alternating Direction Method of Multipliers (tADMM)

3.1 Introduction and Motivation

Multi-period optimal power flow (MPOPF) problems are computationally challenging due to the coupling of variables across time periods through energy storage devices, such as batteries. The temporal coupling arises from the state-of-charge (SOC) dynamics, which link the battery's energy level at each time step to its charging/discharging decisions throughout the entire planning horizon. For large-scale distribution networks with multiple time periods, solving the centralized MPOPF problem becomes intractable.

The Alternating Direction Method of Multipliers (ADMM) is a powerful decomposition technique for solving large-scale convex optimization problems [12, 13]. ADMM is particularly effective for problems that can be decomposed into smaller, more manageable subproblems. The temporal ADMM (tADMM) approach adapts the classical ADMM framework to decompose the MPOPF problem across the temporal dimension, enabling parallel computation of individual time-step subproblems while maintaining consensus on the battery SOC trajectories.

The key insight of tADMM is that while spatial network constraints (power flow equations, voltage limits) are local to each time step, the temporal coupling through battery SOC can be handled through consensus variables. Each time-step subproblem maintains its own local copy of the battery SOC trajectory, and these local copies are coordinated through a global consensus variable that is updated iteratively. This decomposition structure allows for:

- **Parallel computation**: Each time-step subproblem can be solved independently and in parallel
- **Scalability**: Computational complexity grows more favorably with the number of time periods compared to centralized approaches
- **Modularity**: The framework can accommodate different network models (LinDistFlow, copper plate) without changing the decomposition structure

3.2 LinDistFlow MPOPF with tADMM

3.2.1 Problem Overview

The Temporal ADMM (tADMM) algorithm decomposes the multi-period optimal power flow problem for distribution networks into T subproblems, each corresponding to one time period. This formulation uses the linearized DistFlow model to capture network physics including voltage drops and reactive power flows. The algorithm maintains consensus on battery state-of-charge (SOC) trajectories across all subproblems through an iterative update procedure.

3.2.2 Variable Color Coding

To clearly distinguish the different types of variables in the tADMM formulation, we use the following color-coding scheme:

- $\mathbf{B_j^{t_0}[t]}$ (Blue): Local SOC variables for battery j in subproblem t_0, evaluated at time t. These are the primal variables optimized in each subproblem.
- $\mathbf{\hat{B}_j[t]}$ (Red): Global consensus SOC for battery j at time t. This represents the agreed-upon SOC trajectory that all subproblems aim to converge to.
- $\mathbf{u_j^{t_0}[t]}$ (Green): Local scaled dual variables for battery j in subproblem t_0, for time t. These accumulate the consensus violation and guide convergence.

3.2.3 Sets and Indices

- $\mathscr{N}$: Set of all nodes (buses)
- $\mathscr{L}$: Set of all branches (lines)
- $\mathscr{L}_1$: Set of branches connected to substation (node 1)
- $\mathscr{B}$: Set of nodes with batteries
- $\mathscr{D}$: Set of nodes with PV (DER)
- $\mathscr{T} = \{1, 2, \ldots, T\}$: Set of time periods
- $t_0 \in \mathscr{T}$: Index for a specific time period in tADMM decomposition

- $j \in \mathscr{N}$: Node index
- $(i, j) \in \mathscr{L}$: Branch from node i to node j

3.2.4 tADMM Algorithm Structure

The tADMM algorithm follows the consensus-based ADMM framework [12, 13], where the true global problem involves a single consensus variable that is used (partially or fully) by all individual subproblems. In the context of MPOPF, the consensus variable is the battery SOC trajectory, and each time-step subproblem maintains its own local copy of this trajectory.

The algorithm alternates between three update steps at each iteration k:

3.2.4.1 Step 1: Subproblem Update (Blue Variables) In the first update step, we solve each subproblem $t_0 \in \{1, 2, \ldots, T\}$ independently and in parallel. Each subproblem optimizes its local copy of the battery SOC trajectory $\mathbf{B_j^{t_0}[t]}$ along with the network variables for its specific time step. The latest values of the global consensus variable $\mathbf{\hat{B}_j[t]}$ and dual variables $\mathbf{u_j^{t_0}[t]}$ from the previous iteration are used to guide the optimization toward consensus.

For each subproblem $t_0 \in \{1, 2, \ldots, T\}$:

$$\begin{aligned} \min_{\substack{P_{\text{Subs}}^{t_0}, Q_{\text{Subs}}^{t_0}, \\ P_{ij}^{t_0}, Q_{ij}^{t_0}, v_j^{t_0}, q_{D,j}^{t_0}, \\ P_{B,j}^{t}, \mathbf{B_j^{t_0}[t]} \\ \forall j \in \mathscr{B}, t \in \mathscr{T}}} \quad & c^{t_0} \cdot P_{\text{Subs}}^{t_0} \cdot P_{\text{BASE}} \cdot \Delta t + C_B \sum_{j \in \mathscr{B}} \left(P_{B,j}^{t_0}\right)^2 \cdot P_{\text{BASE}}^2 \cdot \Delta t \\ & + \frac{\rho}{2} \sum_{j \in \mathscr{B}} \sum_{t=1}^{T} \left(\mathbf{B_j^{t_0}[t]} - \mathbf{\hat{B}_j[t]} + \mathbf{u_j^{t_0}[t]} \right)^2 \end{aligned} \tag{1}$$

Subject to:

Spatial Network Constraints (only for time t_0):

$$\text{Real power balance (substation):} \quad P^{t_0}_{\text{Subs}} - \sum_{(1,j)\in\mathscr{L}_1} P^{t_0}_{1j} = 0 \tag{2}$$

$$\text{Real power balance (nodes):} \quad P^{t_0}_{ij} - \sum_{(j,k)\in\mathscr{L}} P^{t_0}_{jk} = P^{t_0}_{B,j} + p^{t_0}_{D,j} - p^{t_0}_{L,j}, \quad \forall (i,j) \in \mathscr{L}, \tag{3}$$

$$\text{Reactive power balance (substation):} \quad Q^{t_0}_{\text{Subs}} - \sum_{(1,j)\in\mathscr{L}_1} Q^{t_0}_{1j} = 0 \tag{4}$$

$$\text{Reactive power balance (nodes):} \quad Q^{t_0}_{ij} - \sum_{(j,k)\in\mathscr{L}} Q^{t_0}_{jk} = q^{t_0}_{D,j} - q^{t_0}_{L,j}, \quad \forall (i,j) \in \mathscr{L}, \tag{5}$$

$$\text{KVL constraints:} \quad v^{t_0}_i - v^{t_0}_j = 2(r_{ij}P^{t_0}_{ij} + x_{ij}Q^{t_0}_{ij}), \quad \forall (i,j) \in \mathscr{L} \tag{6}$$

$$\text{Voltage limits:} \quad (V_{\min,j})^2 \le v^{t_0}_j \le (V_{\max,j})^2, \quad \forall j \in \mathscr{N} \tag{7}$$

$$\text{PV reactive limits:} \quad -\sqrt{(S_{D,j})^2 - (p^{t_0}_{D,j})^2} \le q^{t_0}_{D,j} \le \sqrt{(S_{D,j})^2 - (p^{t_0}_{D,j})^2}, \quad \forall j \in \mathscr{D} \tag{8}$$

Temporal Battery Constraints (entire horizon $t \in \{1,\dots,T\}$):

$$\text{Initial SOC:} \quad \mathbf{B^{t_0}_j[1]} = B_{0,j} - P^1_{B,j}\cdot\Delta t, \quad \forall j \in \mathscr{B} \tag{9}$$

$$\text{SOC trajectory:} \quad \mathbf{B^{t_0}_j[t]} = \mathbf{B^{t_0}_j[t-1]} - P^t_{B,j}\cdot\Delta t, \quad \forall t \in \{2,\dots,T\},\ j \in \mathscr{B} \tag{10}$$

$$\text{SOC limits:} \quad \text{SOC}_{\min,j}\cdot B_{\text{rated},j} \le \mathbf{B^{t_0}_j[t]} \le \text{SOC}_{\max,j}\cdot B_{\text{rated},j}, \quad \forall t \in \mathscr{T},\ j \in \mathscr{B} \tag{11}$$

$$\text{Power limits:} \quad -P_{B,\text{rated},j} \le P^t_{B,j} \le P_{B,\text{rated},j}, \quad \forall t \in \mathscr{T},\ j \in \mathscr{B} \tag{12}$$

Key Formulation Notes:

- **Network variables** $(P^{t_0}_{\text{Subs}}, Q^{t_0}_{\text{Subs}}, P^{t_0}_{ij}, Q^{t_0}_{ij}, v^{t_0}_j, q^{t_0}_{D,j})$ are optimized *only* for time step t_0, representing the spatial network state at that particular time
- **Battery power** $P^t_{B,j}$ is optimized for the *entire* horizon $t \in \{1,\dots,T\}$ to allow proper accounting of temporal coupling
- **Local SOC trajectory** $\mathbf{B^{t_0}_j[t]}$ is computed for *all* time steps $t \in \{1,\dots,T\}$ based on the battery power decisions

- The ADMM consensus penalty compares the full local trajectory $\mathbf{B_j^{t_0}[t]}$ with the global master copy $\mathbf{\hat{B}_j[t]}$, penalized by the dual variables $\mathbf{u_j^{t_0}[t]}$
- Each battery $j \in \mathscr{B}$ has its own set of local/global SOC variables and dual variables

3.2.4.2 Step 2: Consensus Update (Red Variables) After all subproblems have been solved in parallel to obtain the latest values of $\mathbf{B_j^{t_0}[t]}$, the global consensus variable $\mathbf{\hat{B}_j[t]}$ is updated by averaging the local SOC trajectories across all subproblems, adjusted by the dual variables. This update brings the consensus closer to the average of what each subproblem believes the SOC should be.

For each battery $j \in \mathscr{B}$ and each time period $t \in \mathscr{T}$:

$$\mathbf{\hat{B}_j[t]} = \text{clamp}\left(\frac{1}{T}\sum_{t_0=1}^{T}\left(\mathbf{B_j^{t_0}[t]} + \mathbf{u_j^{t_0}[t]}\right), \underline{B}_j, \overline{B}_j\right) \tag{13}$$

where $\underline{B}_j = \text{SOC}_{\text{min},j} \cdot B_{\text{rated},j}$ and $\overline{B}_j = \text{SOC}_{\text{max},j} \cdot B_{\text{rated},j}$. The clamping operation ensures that the consensus variable respects the physical SOC bounds.

3.2.4.3 Step 3: Dual Update (Green Variables) Finally, the dual variables $\mathbf{u_j^{t_0}[t]}$ are updated to accumulate the consensus violation (the difference between local and global SOC). These dual variables act as Lagrange multipliers that enforce consensus in the limit as the algorithm converges.

For each battery $j \in \mathscr{B}$, each subproblem $t_0 \in \mathscr{T}$, and each time period $t \in \mathscr{T}$:

$$\mathbf{u_j^{t_0}[t]} := \mathbf{u_j^{t_0}[t]} + \left(\mathbf{B_j^{t_0}[t]} - \mathbf{\hat{B}_j[t]}\right) \tag{14}$$

These three steps are repeated iteratively: solve subproblems for blue variables, update consensus red variables, and update dual green variables, until convergence is achieved.

3.2.5 Convergence Criteria

Primal Residual (Consensus Violation):

The primal residual measures how well the local SOC trajectories $\mathbf{B_j^{t_0}[t]}$ agree with the global consensus $\mathbf{\hat{B}_j[t]}$ across all batteries and time steps.

$$\|r^k\|_2 = \frac{1}{|\mathscr{B}|}\sqrt{\sum_{j\in\mathscr{B}}\sum_{t=1}^{T}\left(\frac{1}{T}\sum_{t_0=1}^{T}\mathbf{B_j^{t_0}[t]} - \mathbf{\hat{B}_j[t]}\right)^2} \leq \epsilon_{\text{pri}} \tag{15}$$

Dual Residual (Consensus Change):

The dual residual measures the change in the consensus variable between iterations, indicating convergence stability.

$$\|s^k\|_2 = \frac{\rho}{|\mathscr{B}|}\sqrt{\sum_{j\in\mathscr{B}}\sum_{t=1}^{T}\left(\mathbf{\hat{B}_j^k[t]} - \mathbf{\hat{B}_j^{k-1}[t]}\right)^2} \leq \epsilon_{\text{dual}} \tag{16}$$

3.3 Copper Plate MPOPF with tADMM (Simplified Case)

3.3.1 Problem Overview

To illustrate the tADMM framework more clearly, we first present a simplified copper plate model where network constraints are neglected, and only a single aggregate power balance is enforced at each time step. The Temporal ADMM (tADMM) algorithm decomposes the multi-period optimal power flow problem into T single-step subproblems, each corresponding to one time period. The hope is to enable parallel computation and improved scalability while still retaining solution optimality. Fig. 1 shows the input data for a 24-hour horizon, including the time-varying electricity cost and load demand profiles used in the copper plate MPOPF formulation.

3.3.2 Variable Color Coding

- $\mathbf{B^{t_0}}$ (Blue): Local SOC variables for subproblem t_0
- $\mathbf{\hat{B}}$ (Red): Global consensus SOC trajectory
- $\mathbf{u^{t_0}}$ (Green): Local scaled dual variables for subproblem t_0

3.3.3 tADMM Algorithm Structure

The algorithm alternates between three update steps following the consensus ADMM framework [12, 13]:

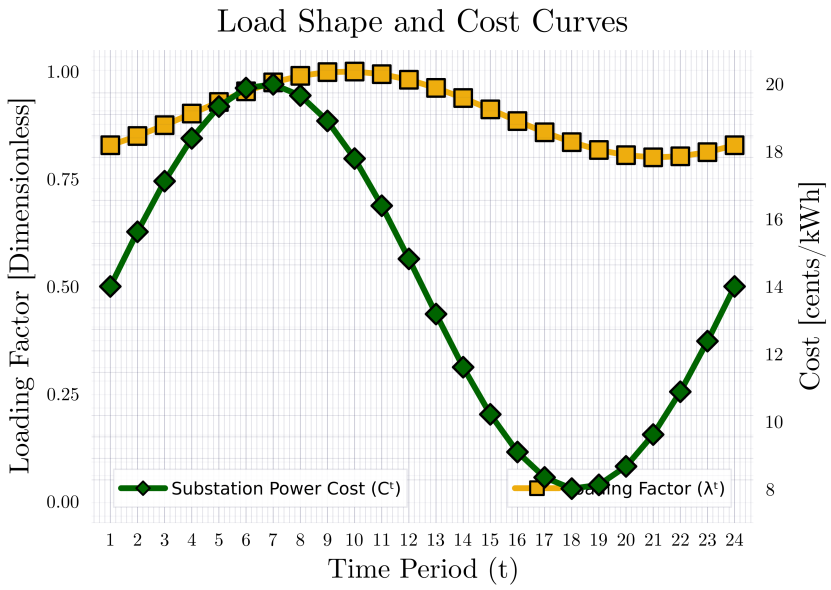

Figure 1: Input curves showing electricity cost and load demand over a 24-hour period.

3.3.3.1 Step 1: Primal Update (Blue Variables) - tADMM Optimization Model

In Update 1 (at iteration k), the latest values of subproblem copies are solved for in parallel using the last known copies of the consensus variable and dual variables – namely $\hat{\mathbf{B}}^{\mathbf{k-1}}$ and $\mathbf{u}^{\mathbf{t_0},\mathbf{k-1}}$, respectively.

For each subproblem $t_0 \in \{1, 2, \ldots, T\}$:

$$\min_{P^{t_0}_{\text{subs}}, P^{t_0}_B, \mathbf{B^{t_0}}} \quad C^{t_0} \cdot P^{t_0}_{\text{subs}} + C_B \cdot \left(P^{t_0}_B\right)^2 + \frac{\rho}{2} \left\| \mathbf{B^{t_0}} - \hat{\mathbf{B}} + \mathbf{u^{t_0}} \right\|_2^2 \tag{17}$$

Subject to SOC Dynamics for Entire Trajectory:

$$\mathbf{B^{t_0}[1]} = B_0 - P^{t_0}_B \cdot \Delta t \tag{18}$$

$$\mathbf{B^{t_0}[t]} = \mathbf{B^{t_0}[t-1]} - P^{t_0}_B \cdot \Delta t, \quad \forall t \in \{2, \ldots, T\} \tag{19}$$

$$P^{t_0}_{\text{subs}} + P^{t_0}_B = P_L[t_0] \tag{20}$$

$$-P_{B,R} \leq P^{t_0}_B \leq P_{B,R} \tag{21}$$

$$\underline{B} \leq \mathbf{B^{t_0}[t]} \leq \overline{B}, \quad \forall t \in \{1, \ldots, T\} \tag{22}$$

Key Formulation Notes:

- Each subproblem t_0 optimizes the battery power $P_B^{t_0}$ for *only* time step t_0
- However, the SOC trajectory $\mathbf{B^{t_0}[t]}$ is computed for *all* time steps $t \in \{1, \ldots, T\}$
- This ensures that the ADMM penalty term can compare the full trajectory $\mathbf{B^{t_0}}$ with the consensus $\hat{\mathbf{B}}$
- The power balance constraint is enforced only for the specific time t_0

3.3.3.2 Step 2: Consensus Update (Red Variables) In Update 2 (at iteration k), the latest value of the global consensus variable is computed using the last known copies of the local subproblem SOC trajectories and dual variables – namely $\mathbf{B_i^{t_0,k}}$ and $\mathbf{u_i^{t_0,k-1}}$, respectively.

$$\hat{\mathbf{B}}[\mathbf{t}] = \text{clamp}\left(\frac{1}{T}\sum_{t_0=1}^{T}\left(\mathbf{B^{t_0}[t]} + \mathbf{u^{t_0}[t]}\right), \underline{B}, \overline{B}\right) \tag{23}$$

$$\forall t \in \{1, 2, \ldots, T-1\} \tag{24}$$

$$\hat{\mathbf{B}}[\mathbf{T}] = B_{T,\text{target}} \quad \text{(if terminal constraint exists)} \tag{25}$$

3.3.3.3 Step 3: Dual Update (Green Variables) In Update 3 (at iteration k), the latest values of local dual variables are computed using the last known copies of the local SOC, global consensus, and previous dual variables – namely $\mathbf{B_i^{t_0,k}}$, $\hat{\mathbf{B}}^{\mathbf{k}}$, and $\mathbf{u_i^{t_0,k-1}}$, respectively.

$$\mathbf{u^{t_0}[t]} := \mathbf{u^{t_0}[t]} + \left(\mathbf{B^{t_0}[t]} - \hat{\mathbf{B}}[\mathbf{t}]\right) \tag{26}$$

$$\forall t_0 \in \{1, \ldots, T\}, \forall t \in \{1, \ldots, T\} \tag{27}$$

After every subproblem is solved once to get the latest values of $\mathbf{B_1}, \mathbf{B_2}, \ldots, \mathbf{B_B}$, the value of the consensus variable $\hat{\mathbf{B}}$ is updated. Next, the dual variables $\mathbf{u_1}, \mathbf{u_2}, \ldots, \mathbf{u_B}$ are updated. This process repeats until convergence.

3.4 Numerical Results

3.4.1 Battery Actions and Convergence Analysis

To validate the tADMM approach, we present numerical results for the copper plate MPOPF problem with a 24-hour planning horizon. The test case includes a single battery energy storage system with time-varying electricity prices and load demands as shown in Fig. 1.

Fig. 2 shows the optimal battery charging and discharging actions obtained from solving the centralized (brute force) MPOPF problem. The battery strategically charges during low-cost periods (typically during nighttime and early morning hours) and discharges during high-cost periods (peak demand hours in the afternoon and evening) to minimize the overall energy cost over the 24-hour horizon. This behavior demonstrates the value of energy arbitrage enabled by battery storage.

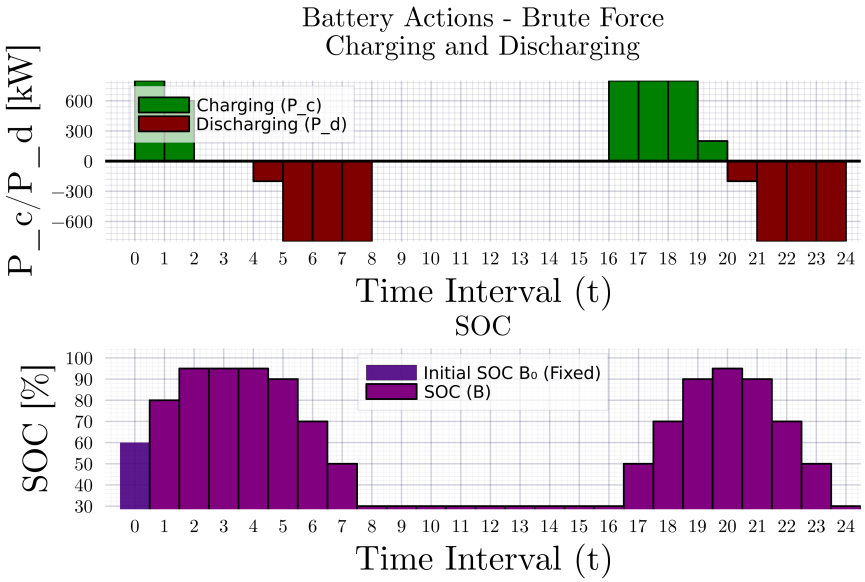

Figure 2: Optimal battery power actions (brute force centralized solution) for copper plate MPOPF over 24-hour horizon. Positive values indicate discharging (supplying power), while negative values indicate charging (consuming power).

Fig. 3 presents the battery actions obtained using the tADMM algorithm, demonstrating that the decomposition approach converges to a solution that closely matches the centralized optimal solution. The close agreement between the two solutions validates the effectiveness of the tADMM decomposition for this problem class. Minor differences, if any, are within the specified convergence tolerances.

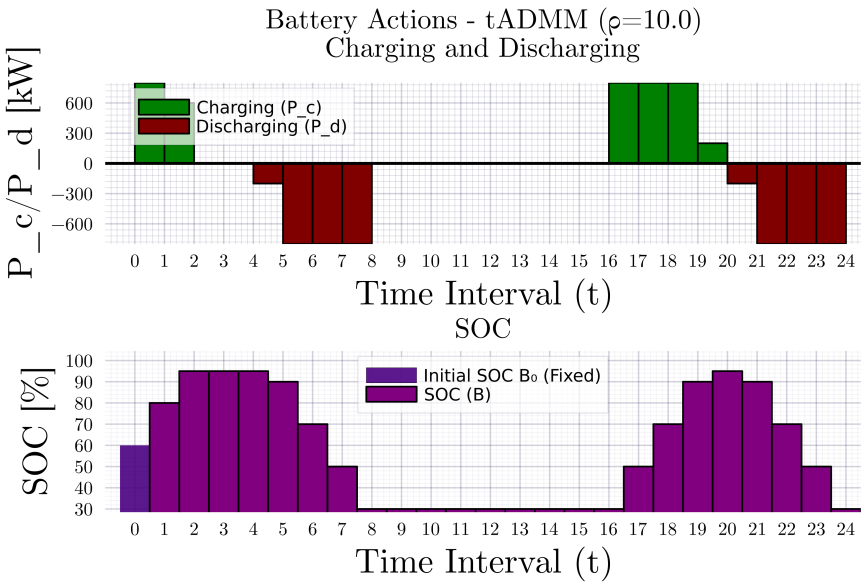

Figure 3: Battery power actions obtained using tADMM for copper plate MPOPF over 24-hour horizon. The solution converges to match the centralized optimal solution.

Fig. 4 illustrates the convergence behavior of the tADMM algorithm, showing how the primal and dual residuals decrease over iterations until they satisfy the specified convergence tolerances ($\epsilon_{\text{pri}} = 10^{-3}$ and $\epsilon_{\text{dual}} = 10^{-3}$). The algorithm typically converges within a few dozen iterations, demonstrating good computational efficiency. The primal residual (consensus violation) decreases as the local SOC trajectories $\mathbf{B}^{\mathbf{t_0}}$ converge to the global consensus $\hat{\mathbf{B}}$, while the dual residual tracks the stability of the consensus variable across iterations.

3.5 Convergence Criteria

The algorithm terminates when both residuals fall below specified thresholds:

3.5.1 Convergence Criteria

The algorithm terminates when both residuals fall below specified thresholds:

Primal Residual (Consensus Violation):

The primal residual measures how well the local SOC trajectories $\mathbf{B}^{\mathbf{t_0}}$ agree with the global consensus $\hat{\mathbf{B}}$. A small primal residual indicates that all subproblems have converged to a consistent SOC trajectory.

$$\|r^k\|_2 = \left\| \text{vec} \left(\left\{ \mathbf{B^{t_0}} - \hat{\mathbf{B}} \right\}_{t_0=1}^{T} \right) \right\|_2 \leq \epsilon_{\text{pri}} \tag{28}$$

Dual Residual (Consensus Change):

The dual residual measures how much the consensus variable $\hat{\mathbf{B}}$ is changing between iterations. A small dual residual indicates that the consensus has stabilized.

$$\|s^k\|_2 = \rho \left\| \hat{\mathbf{B}}^{\mathbf{k}} - \hat{\mathbf{B}}^{\mathbf{k-1}} \right\|_2 \leq \epsilon_{\text{dual}} \tag{29}$$

3.6 Algorithm Parameters

3.6.1 Objective Function Components

The tADMM objective function for each subproblem t_0 consists of three terms:

$$\text{Energy Cost:} \quad C^{t_0} \cdot P_{\text{subs}}^{t_0} \cdot \Delta t \tag{30}$$

$$\text{Battery Quadratic Cost:} \quad C_B \cdot \left(P_B^{t_0}\right)^2 \cdot \Delta t \tag{31}$$

$$\text{ADMM Penalty:} \quad \frac{\rho}{2} \left\| B^{t_0} - \hat{B} + u^{t_0} \right\|_2^2 \tag{32}$$

Where:

- C^{t_0}: Energy price at time t_0 [\$/kWh]
- C_B: Battery quadratic cost coefficient [\$/kW^2/h] (typically $10^{-6} \times \min(C^t)$)
- ρ: ADMM penalty parameter

The battery quadratic cost term $C_B \cdot \left(P_B^{t_0}\right)^2$ serves as a regularization to:

1. Prevent excessive battery cycling
2. Encourage smoother power trajectories
3. Improve numerical conditioning of the optimization problem

3.6.2 Algorithmic Parameters

- **Penalty Parameter**: ρ (typically 0.1 to 10.0)
- **Primal Tolerance**: $\epsilon_{\text{pri}} = 10^{-3}$
- **Dual Tolerance**: $\epsilon_{\text{dual}} = 10^{-3}$
- **Maximum Iterations**: 1000

3.7 Appendix: Full Variable and Parameter Definitions

3.7.1 System Bases

$$\text{kV}_B = \frac{4.16}{\sqrt{3}} \text{ kV (phase-to-neutral)} \tag{33}$$

$$\text{kVA}_B = 1000 \text{ kVA} \tag{34}$$

$$P_{\text{BASE}} = 1000 \text{ kW} \tag{35}$$

$$E_{\text{BASE}} = 1000 \text{ kWh per hour} \tag{36}$$

3.7.2 SOC Bound Definitions

$$\underline{B} = \text{SOC}_{\min} \cdot E_{\text{Rated}} \tag{37}$$

$$\overline{B} = \text{SOC}_{\max} \cdot E_{\text{Rated}} \tag{38}$$

3.7.3 Physical Interpretation

- $P_B[t] > 0$: Battery discharging (providing power to the system)
- $P_B[t] < 0$: Battery charging (consuming power from the system)
- $B[t]$: Battery state of charge at the end of period t
- $\underline{B} = \text{SOC}_{\min} \cdot E_{\text{Rated}}$: Lower SOC bound
- $\overline{B} = \text{SOC}_{\max} \cdot E_{\text{Rated}}$: Upper SOC bound

3.8 Summary and Discussion

The temporal ADMM (tADMM) approach provides an effective decomposition framework for solving multi-period optimal power flow problems with energy storage. The key advantages of this approach include:

- **Parallelization**: Each time-step subproblem can be solved independently and in parallel, enabling computational speedup on multi-core processors or distributed computing platforms
- **Modularity**: The decomposition structure is flexible and can accommodate different network models (LinDistFlow, AC power flow, copper plate) without changing the temporal decomposition framework
- **Scalability**: The computational complexity scales more favorably with the number of time periods compared to solving the full centralized problem
- **Convergence guarantees**: For convex formulations, ADMM provides theoretical convergence guarantees to the global optimum [12, 13]

The numerical results demonstrate that tADMM successfully decomposes the temporal coupling through battery SOC while maintaining solution optimality. The algorithm converges within a reasonable number of iterations, and the final solution matches the centralized optimal solution within the specified tolerances. This validates the effectiveness of the consensus-based decomposition for handling temporal coupling in MPOPF problems.

3.8.1 Implementation Status

The tADMM framework has been developed and tested with varying levels of network model complexity:

- **Copper Plate Model (Completed)**: The tADMM algorithm has been successfully implemented and tested for the simplified copper plate MPOPF problem. The numerical results presented in Figs. 2, 3, and 4 demonstrate successful convergence to the optimal solution, validating the temporal decomposition approach.
- **LinDistFlow Model (In Progress)**: The tADMM formulation with the linearized DistFlow model [14] is currently being implemented. This will incorporate spatial

network constraints including voltage limits, line flow limits, and reactive power constraints while maintaining the temporal decomposition structure.

- **Nonlinear Branch Flow Model (Planned)**: Future work will extend the tADMM framework to the SOCP-relaxed nonlinear branch flow model (BFM) [4]. This represents the true nonlinear MPOPF problem with exact AC power flow physics. The BFM formulation will provide a more accurate representation of distribution network behavior while benefiting from the computational advantages of temporal decomposition. This will showcase the full potential of tADMM for solving realistic large-scale MPOPF problems with complex network constraints.

Future extensions of this work will focus on:

- Completing the LinDistFlow implementation and validating performance on realistic distribution networks
- Implementing the SOCP-relaxed BFM formulation with tADMM decomposition
- Applying tADMM to larger distribution networks with multiple batteries and renewable energy sources
- Investigating adaptive penalty parameter selection strategies to improve convergence speed
- Integrating spatial decomposition techniques with temporal decomposition for enhanced scalability

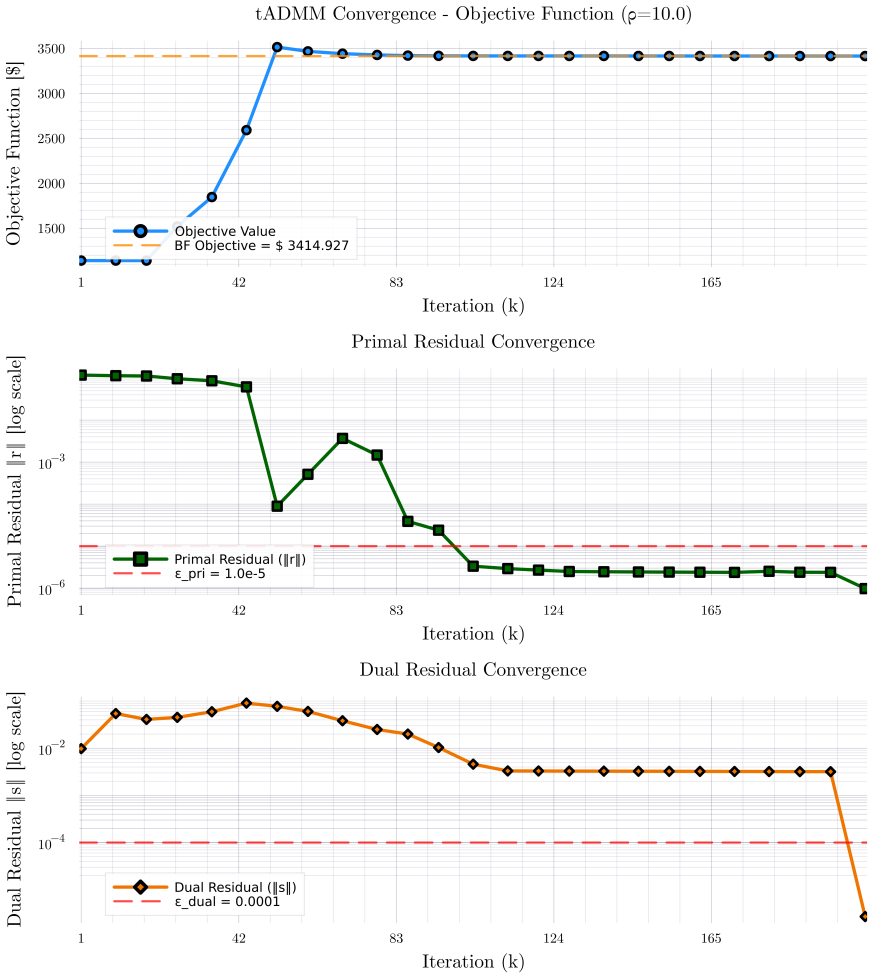

Figure 4: Convergence curves showing primal and dual residuals for tADMM algorithm. Both residuals decrease monotonically and satisfy the convergence criteria.

4 Future Works

The proposed future work aims to extend the temporal decomposition framework developed in this research to larger and more complex power distribution systems. The timeline for completion spans three semesters from Fall 2025 through Summer 2026, culminating in dissertation preparation and defense. The work is organized into three main tasks that progressively scale the methodology and conclude the doctoral research.

4.1 Task 1: Temporal Decomposition for Medium Sized Balanced Three-Phase Systems

The first task focuses on developing and validating the temporal decomposition approach for medium-scale distribution systems assuming balanced three-phase conditions. So far the mathematical framework for temporal decomposition using tADMM has been established, extending the concepts developed in earlier work to handle time-coupled constraints and multi-period optimization problems. The formulation phase will establish the theoretical foundations and decomposition strategy.

Following the formulation, implementation and testing will be conducted on the IEEE 123-bus single-phase test system. This medium-scale system provides sufficient complexity to validate the decomposition approach while remaining computationally tractable for initial testing. The implementation will focus on developing efficient algorithms and testing convergence properties. This task is scheduled for completion during Fall 2025.

4.2 Task 2: Temporal Decomposition for Large Sized Unbalanced Three-Phase Systems

The second task scales the temporal decomposition methodology to large-scale three-phase distribution systems. Building on the insights from Task 1, this phase will formulate the decomposition approach specifically for three-phase unbalanced systems, accounting for the additional complexity of phase coupling and imbalance.

The implementation and testing will be performed on the IEEE 9500-bus three-phase test system, which represents a realistic large-scale distribution network. This task will demonstrate the scalability of the temporal decomposition approach and validate its effectiveness on industry-relevant system sizes. The work is planned for completion during Spring 2026.

4.3 Task 3: Concluding Research and Dissertation

The final task encompasses completion of remaining research activities and dissertation preparation. This includes finishing the investigation of differential dynamic programming (DDP) methods, conducting a comprehensive literature review on novel temporal decomposition methods in power systems, and completing any remaining implementations or case studies.

The dissertation preparation and defense phase will synthesize all research contributions, document the methodologies and results, and prepare for the final defense. This task spans from late Spring 2026 through Summer 2026, concluding the doctoral research program.

4.4 Timeline

The timeline for the research efforts as detailed in Section 4 is shown in Fig. 5.

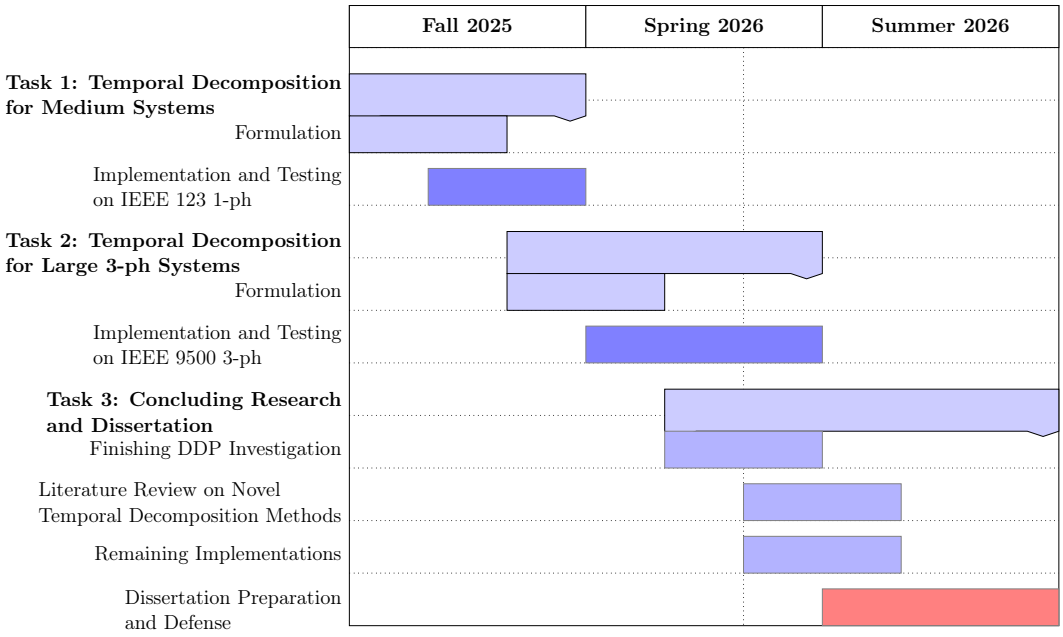

Figure 5: Gantt chart showing execution plan for future works.

5 Biography

Aryan Ritwajeet Jha received the B.E. degree in Electrical and Electronics Engineering from the Birla Institute of Technology and Science (BITS) Pilani, India, in 2020. He is currently pursuing his Ph.D. in Electrical Engineering at Washington State University, Pullman, WA, USA. His research interests include power distribution system optimization, scalable decomposition algorithms for large-scale non-linear optimization and optimization solvers.

5.1 Publications

1. **Jha, A. R.**, Paul, S., & Dubey, A. . Spatially Distributed Multi-Period Optimal Power Flow with Battery Energy Storage Systems. 2024 56th North American Power Symposium (NAPS). IEEE. doi: 10.1109/NAPS61145.2024.10741846 [1]

2. **Jha, A. R.**, Paul, S., & Dubey, A. . Analyzing the Performance of Linear and Nonlinear Multi -Period Optimal Power Flow Models for Active Distribution Networks. 2025 IEEE North-East India International Energy Conversion Conference and Exhibition (NE-IECCE). IEEE. doi: 10.1109/NE-IECCE64154.2025.11183479 [8]

5.2 Program of Study Course Work

Course Number and Name	Semester	Instructor	Grade
E_E 507 Random Processes in Engineering	Fall 2022	Prof. Sandip Roy	A
E_E 521 Analysis of Power Systems	Fall 2022	Prof. Noel Schulz	A
E_E 523 Power Systems Stability	Spring 2023	Prof. Mani V. Venkatasubramanian	A
MATH 564 Convex and Nonlinear Optimization	Fall 2023	Prof. Tom Asaki	A
MATH 565 Nonsmooth Analysis and Optimization	Spring 2024	Prof. Tom Asaki	A-
CPT_S 530 Numerical Analysis[1]	Fall 2025	Prof. Alexander Panchenko	
E_E 582 Electrical Systems Modelling and Simulation[1]	Fall 2025	Prof. Seyedmilad Ebrahimi	
E_E 595 Directed Studies in Electrical Engineering[1]	Fall 2025	Prof. Rahul K. Gupta	

1

[1] currently taking this semester

Appendix

In Section .1 from Equations (39) to (51), the full optimization formulation for the Multi-Period Optimal Power Flow (MPOPF) problem using the LinDistFlow model is presented.

.1 Full MPOPF Formulation with LinDistFlow

Sets:

- $\mathbb{N}$: Set of all buses, with substation bus $j_1 \in \mathbb{N}$
- $\mathbb{N}\backslash\{j_1\}$: Set of non-substation buses
- $\mathbb{L}$: Set of all branches (directed edges)
- $\mathbb{L}_1$: Set of branches directly connected to substation bus j_1
- $\mathbb{L}\backslash\mathbb{L}_1$: Set of branches not connected to substation
- $\mathbb{B}$: Set of buses with battery storage
- $\mathbb{D}$: Set of buses with distributed energy resources (DERs)
- $\mathbb{T}$: Set of time periods $\{1, 2, \ldots, T\}$

Objective Function:

$$\min \quad \sum_{t\in\mathbb{T}} C^t P^t_{\text{Subs}} \Delta t + \sum_{t\in\mathbb{T}} \sum_{j\in\mathbb{B}} C_B (P^t_{B_j})^2 \Delta t \tag{39}$$

Subject to:
Power Balance at Substation Bus ($j = j_1$):

$$P^t_{\text{Subs}} - \sum_{(j_1,k)\in\mathbb{L}_1} P^t_{j_1 k} = 0, \quad \forall t \in \mathbb{T} \tag{40}$$

$$Q^t_{\text{Subs}} - \sum_{(j_1,k)\in\mathbb{L}_1} Q^t_{j_1 k} = 0, \quad \forall t \in \mathbb{T} \tag{41}$$

Power Balance at Non-Substation Buses ($j \in \mathbb{N}\backslash\{j_1\}$):

$$\sum_{(j,k)\in\mathbb{L}} P^t_{jk} - \sum_{(i,j)\in\mathbb{L}} P^t_{ij} = P^t_{B_j} + p^t_{D_j} - p^t_{L_j}, \quad \forall j \in \mathbb{N}, \forall t \in \mathbb{T} \tag{42}$$

$$\sum_{(j,k)\in\mathbb{L}} Q^t_{jk} - \sum_{(i,j)\in\mathbb{L}} Q^t_{ij} = q^t_{D_j} - q^t_{L_j}, \quad \forall j \in \mathbb{N}, \forall t \in \mathbb{T} \tag{43}$$

Voltage Drop (LinDistFlow KVL):

$$v_j^t = v_i^t - 2(r_{ij}P_{ij}^t + x_{ij}Q_{ij}^t), \quad \forall (i,j) \in \mathbb{L}, \forall t \in \mathbb{T} \tag{44}$$

Substation Voltage:

$$v_{j_1}^t = v_{\text{nom}}^2, \quad \forall t \in \mathbb{T} \tag{45}$$

Voltage Limits:

$$(v_{\min})^2 \leq v_j^t \leq (v_{\max})^2, \quad \forall j \in \mathbb{N}, \forall t \in \mathbb{T} \tag{46}$$

Battery State of Charge:

$$B_j^t = B_j^{t-1} - P_{B_j}^t \Delta t, \quad \forall j \in \mathbb{B}, \forall t \in \mathbb{T} \backslash \{1\} \tag{47}$$

$$B_j^1 = B_{j,0}, \quad \forall j \in \mathbb{B} \tag{48}$$

Battery Constraints:

$$\text{SOC}_{\min} B_{R_j} \leq B_j^t \leq \text{SOC}_{\max} B_{R_j}, \quad \forall j \in \mathbb{B}, \forall t \in \mathbb{T} \tag{49}$$

$$-P_{B_{R_j}} \leq P_{B_j}^t \leq P_{B_{R_j}}, \quad \forall j \in \mathbb{B}, \forall t \in \mathbb{T} \tag{50}$$

PV Reactive Power Limits:

$$-\sqrt{S_{D_{R_j}}^2 - (p_{D_j}^t)^2} \leq q_{D_j}^t \leq \sqrt{S_{D_{R_j}}^2 - (p_{D_j}^t)^2}, \quad \forall j \in \mathbb{D}, \forall t \in \mathbb{T} \tag{51}$$

Variables:

- $P_{\text{Subs}}^t, Q_{\text{Subs}}^t$: Substation real and reactive power at time t
- P_{ij}^t, Q_{ij}^t: Sending-end real and reactive power flow on branch (i,j) at time t
- v_j^t: Squared voltage magnitude at bus j at time t
- $P_{B_j}^t$: Battery power at bus j at time t (positive = discharging)
- B_j^t: Battery state of charge at bus j at time t
- $q_{D_j}^t$: PV reactive power injection at bus j at time t

Parameters:

- C^t: Energy cost at time t (\$/kWh)
- C_B: Battery degradation cost coefficient
- Δt: Time step duration

- r_{ij}, x_{ij}: Branch resistance and reactance
- $p^t_{L_j}, q^t_{L_j}$: Load real and reactive power at bus j at time t
- $p^t_{D_j}$: PV real power generation at bus j at time t
- $B_{R_j}, P_{B_{R_j}}$: Battery energy and power capacity at bus j
- $S_{D_{R_j}}$: PV apparent power capacity at bus j

References

[1] A. R. Jha, S. Paul, and A. Dubey, "Analyzing the Performance of Linear and Nonlinear Multi - Period Optimal Power Flow Models for Active Distribution Networks," *Published in: 2025 IEEE North-East India International Energy Conversion Conference and Exhibition (NE-IECCE)*, pp. 04–06.

[2] N. Nazir, P. Racherla, and M. Almassalkhi, "Optimal multi-period dispatch of distributed energy resources in unbalanced distribution feeders," *arXiv*, Jun. 2019.

[3] A. Agarwal and L. Pileggi, "Large Scale Multi-Period Optimal Power Flow With Energy Storage Systems Using Differential Dynamic Programming," *IEEE Trans. Power Syst.*, vol. 37, no. 3, pp. 1750–1759, Sep. 2021.

[4] M. Farivar and S. H. Low, "Branch Flow Model: Relaxations and Convexification—Part I," *IEEE Trans. Power Syst.*, vol. 28, no. 3, pp. 2554–2564, Apr. 2013.

[5] A. Gabash and P. Li, "Active-reactive optimal power flow in distribution networks with embedded generation and battery storage," *IEEE Trans. Power Syst.*, vol. 27, no. 4, pp. 2026–2035, Nov. 2012.

[6] N. Nazir and M. Almassalkhi, "Receding-Horizon Optimization of Unbalanced Distribution Systems with Time-Scale Separation for Discrete and Continuous Control Devices," *2018 Power Systems Computation Conference (PSCC)*, pp. 1–7, Jun. 2018.

[7] L. Gan, U. Topcu, and S. H. Low, "Convex Relaxation of Optimal Power Flow Part I: Formulations and Equivalence," in *IEEE Transactions on Power Systems*, 2015, vol. 30, no. 1, pp. 290–301.

[8] A. R. Jha, S. Paul, and A. Dubey, "Spatially Distributed Multi-Period Optimal Power Flow with Battery Energy Storage Systems," *Published in: 2024 56th North American Power Symposium (NAPS)*, pp. 13–15.

[9] G. Valverde, E. M. G. de Oliveira, A. M. V. de Lara, J. R. S. Peres, and N. Favilla, "Multiperiod optimum power flow for active distribution networks incorporating distributed generation and energy storage systems," *IEEE Transactions on Industry Applications*, 2021. [Online]. Available: https://ieeexplore.ieee.org/document/9502092/

[10] A. G. B. et al., "Large scale multi-period optimal power flow with energy storage," *IEEE Transactions on Power Systems*, 2021. [Online]. Available: https://ieeexplore.ieee.org/document/9549701/

[11] ——, "Large scale multi-period optimal power flow with energy storage," *IEEE Transactions on Power Systems*, 2021. [Online]. Available: https://ieeexplore.ieee.org/document/9549701/

[12] "ADMM," Oct. 2025, [Online; accessed 28. Oct. 2025]. [Online]. Available: https://stanford.edu/~boyd/admm.html

[13] "Index of /~ryantibs/convexopt-F16/lectures," Oct. 2025, [Online; accessed 28. Oct. 2025]. [Online]. Available: https://www.stat.cmu.edu/~ryantibs/convexopt-F16/lectures

[14] M. E. Baran and F. F. Wu, "Optimal capacitor placement on radial distribution systems," *IEEE Transactions on Power Delivery*, vol. 4, no. 1, pp. 725–734, 1989.